Protein Science (1998), 7:782–788. Cambridge University Press. Printed in the USA.

The N-terminal segment of antithrombin acts as a steric gate for the binding of heparin

HAZEL L. FITTON, RICHARD SKINNER, TIMOTHY R. DAFFORN, LEI JIN, AND ROBERT N. PIKE[1]

Department of Haematology, University of Cambridge, MRC Centre, Hills Road, Cambridge, CB2 2QH, United Kingdom

(RECEIVED October 8, 1997; ACCEPTED December 4, 1997)

Abstract

The binding of heparin causes a conformational change in antithrombin to give an increased heparin binding affinity and activate the inhibition of thrombin and factor Xa. The areas of antithrombin involved in binding heparin and stabilizing the interaction in the high-affinity form have been partially resolved through the study of both recombinant and natural variants. The role of a section of the N-terminal segment of antithrombin, residues 22–46 (segment 22–46), in heparin binding was investigated using rapid kinetic analysis of the protein cleaved at residues 29–30 by limited proteolysis with thermolysin. The cleaved antithrombin had 5.5-fold lowered affinity for heparin pentasaccharide and 1.8-fold for full-length, high-affinity heparin. It was shown that, although the initial binding of heparin is slightly enhanced by the cleavage, it dissociates much faster from the cleaved form, giving rise to the overall decrease in heparin affinity. This implies that the segment constituting residues 22–46 in the N terminus of antithrombin hinders access to the binding site for heparin, hence the increased initial binding for the cleaved form, whereas, when heparin is bound, segment 22–46 is involved in the stabilization of the binding interaction, as indicated by the increased dissociation constant. When the heparin pentasaccharide is bound to antithrombin prior to incubation with thermolysin, it protects the N-terminal cleavage site, implying that segment 22–46 moves to interact with heparin in the conformational change and thus stabilizes the complex.

Keywords: antithrombin; heparin; kinetic analysis; N-terminal segment; thermolysin

Antithrombin, a plasma serpin (Hunt & Dayhoff, 1980; Olson & Bjork, 1992), plays a major role in the regulation of coagulation, principally as an inhibitor of the serine proteinases thrombin and factor Xa. It differs from most serpins in that its inhibitory activity is limited, due to its reactive site loop being partly inserted into the A β-sheet of the body of the molecule (Carrell et al., 1994; Schreuder et al., 1994; Skinner et al., 1997). Full inhibitory activity is attained upon interaction of antithrombin with the sulfated polysaccharide, heparin (Choay et al., 1983). Recent crystallographic structures (Jin et al., 1997) have provided details of the binding to antithrombin of the core pentasaccharide fragment of heparin. Although these structures give a detailed picture of the binding of the pentasaccharide to the D-helix and associated secondary structures on the body of the molecule, there is an incomplete view of the interaction of the pentasaccharide with the 45-residue N-terminal extension of antithrombin. In these structures (Jin et al., 1997), the first 25 residues of the N terminus are evident, together with the sequence just prior to the A-helix (39–45), but residues 26–38 are not defined. This is also found in all other crystallographic studies to date (Carrell et al., 1994; Schreuder et al., 1994; Skinner et al., 1997) and presumably reflects the flexible and mobile nature of the N-terminal extension. These structures do, however, indicate that the visible section of the peptide loop, residues 39–45, has moved to allow access of the pentasaccharide to the D-helix.

Here we have studied the effects of cleavage of the N terminus, between residues 29 and 30, on the binding of the pentasaccharide and full-length high-affinity heparin. We independently conclude that the N terminus acts as a steric gate to the binding site, initially hindering access and then stabilizing the complex once entry to the binding site has been gained.

Reprint requests to: Hazel L. Fitton, Department of Haematology, University of Cambridge, MRC Centre, Hills Road, Cambridge, CB2 2QH, United Kingdom; e-mail: hlb21@cus.cam.ac.uk.

[1]Present address: Department of Biochemistry and Molecular Biology, Monash University, Clayton, Victoria, 3168, Australia.

Abbreviations: NTC-antithrombin, N-terminally cleaved antithrombin; PVDF, polyvinylidene difluoride; S2222, N-benzoyl-L-isoleucyl-L-glutamyl-glycyl-L-arginine-*p*-nitroaniline hydrochloride and its methyl ester; S2238, H-D-Phenylalanyl-L-pipecolyl-L-arginine-*p*-nitroaniline hydrochloride.

Results

Proteolysis of antithrombin

Antithrombin cleaved by thermolysin eluted from heparin-Sepharose in three peaks, of which only peaks II and III had inhibitory activity against thrombin (Fig. 1). N-terminal sequencing showed the

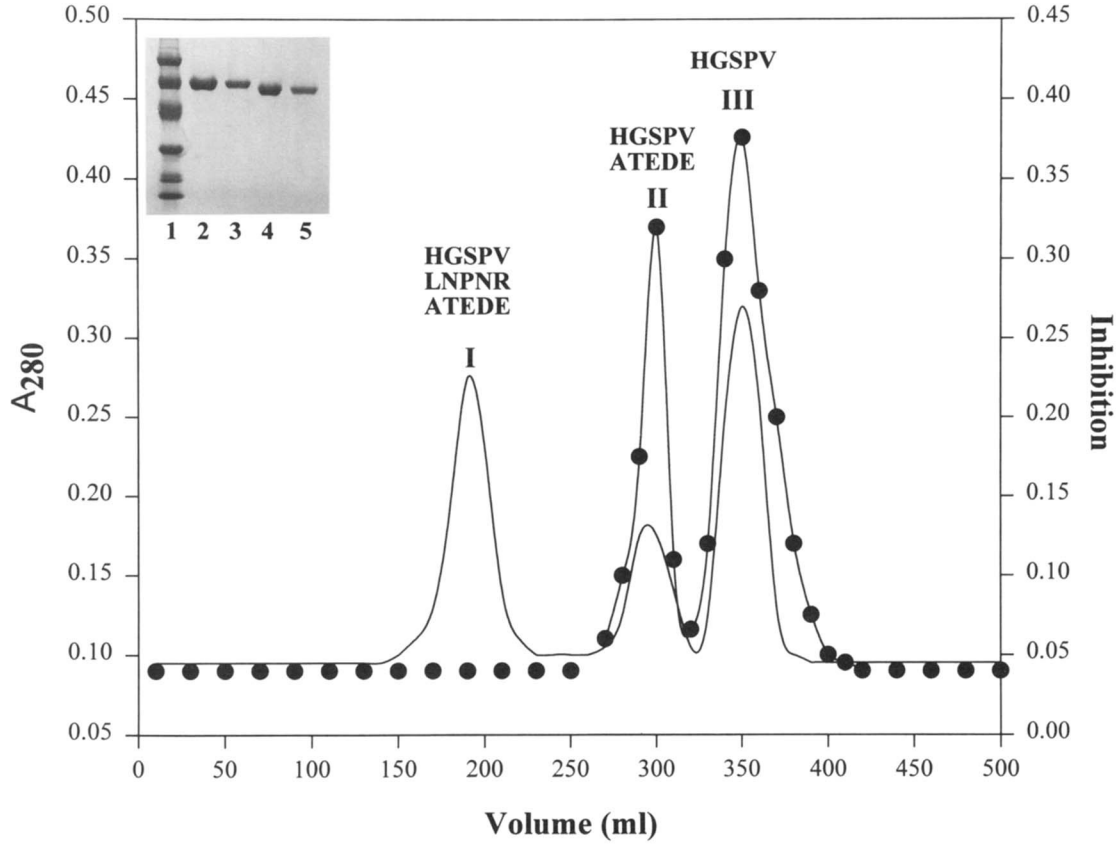

Fig. 1. Heparin-Sepharose chromatography of antithrombin cleaved by thermolysin and reducing SDS-PAGE of NTC- and intact antithrombin. Antithrombin incubated with thermolysin was applied to a heparin-Sepharose column and eluted using a linear 0–2 M NaCl gradient. Fractions were monitored for the presence of protein by the absorbance at 280 nm and assayed for activity against thrombin (●) in I0.15 sodium phosphate buffer, pH 7.4, at 25 °C. N-terminal sequencing of the three forms revealed the native N terminus to be present in each form (HGSPV), with the N-terminal segment cleaved at Lys 29 (ATEDE) in peaks I and II and the reactive site loop cleaved at P_1'-P_2' (LNPNR) in peak I. Therefore, peak I: N-terminally and reactive site loop-cleaved antithrombin; peak II: NTC antithrombin; peak III: intact antithrombin. Inset: SDS-PAGE of purified forms from the heparin-Sepharose. Lane 1, molecular mass markers (phosphorylase *b*, 97 kDa; bovine serum albumin, 68 kDa; ovalbumin, 43 kDa; carbonic anhydrase, 30 kDa; soybean trypsin inhibitor, 20 kDa; α-lactalbumin, 14 kDa); lane 2, 2.5 mg intact antithrombin; lane 3, 1 mg intact antithrombin; lane 4, 2.5 mg NTC-antithrombin; lane 5, 1 mg NTC-antithrombin.

single native N-terminal sequence to be present in the third peak (III), indicating that this was uncleaved, native antithrombin. The second peak (II) showed an additional sequence commencing at alanine 30, indicating cleavage between lysine 29 and alanine 30, whereas sequencing of the first peak (I) showed cleavage both at this position and the reactive site loop bond (P_1'-P_2'), previously shown to be hydrolyzed by thermolysin (Chang et al., 1996). When cleavage experiments were performed in the presence of heparin pentasaccharide, N-terminal sequencing of the products showed that cleavage only occurred at the reactive site loop, suggesting that the lysine 29–alanine 30 site is protected by binding of the pentasaccharide. N-terminal sequencing of the three peaks will only show the most C-terminal cleavage point and not if there is a second cleavage site after cysteine 21, which forms an anchoring disulfide bridge, resulting in the loss of a small peptide from the N-terminal segment. Therefore, the three purified samples were analyzed by mass spectrometry, which showed that peak I has a mass of 57,473, peak II has a mass of 57,552, and peak III has a mass of 57,501, with a standard error of 200 Da. These results indicate that the masses of the two cleaved forms of antithrombin were the same as the intact form of antithrombin, proving that cleavage occurs only at the sites shown by N-terminal sequencing, with the resulting peptides held onto the body of the molecule by disulfide bonds. Peak II (designated NTC-antithrombin) was used for further studies in comparison to native antithrombin.

Characterization of NTC-antithrombin

The overall conformational change in antithrombin induced by heparin binding was quantified by measuring the accompanying increase in fluorescence emission. This showed that the percentage change in emission at the peak of the scan (340 nm) on the addition of pentasaccharide was 27.7 ± 1.0% for NTC-antithrombin, whereas that for intact antithrombin was 36.1 ± 1.1% (data not shown). The second-order rate constant for the association of NTC-antithrombin with factor Xa was found to be indistinguishable from that for intact antithrombin, as was that for the interaction in the presence of pentasaccharide.

Overall affinity of NTC-antithrombin for heparin

The affinity of NTC-antithrombin for heparin pentasaccharide and high-affinity heparin was measured using equilibrium binding titrations obtained by monitoring changes in the intrinsic fluorescence of the protein on addition of the heparins (Olson et al., 1993). As shown in Table 1, the K_d for pentasaccharide binding to NTC-antithrombin increased approximately 5.5-fold, and that for high-affinity heparin increased twofold compared to that for binding to intact antithrombin, at an ionic strength of 0.15 (I0.15). At an ionic strength of 0.3 (I0.3), the K_d for pentasaccharide binding to NTC-antithrombin increased 2.7-fold over that for binding to intact antithrombin, whereas for high-affinity heparin, binding the K_d increased fivefold. The equilibrium dissociation constants were used to calculate the differences in the free energy of binding for NTC-antithrombin compared to normal antithrombin (Table 1). This revealed that there is a loss of approximately 7–10% of the binding energy for the pentasaccharide, assuming a total ΔG_b of -33.4 kJ mol^{-1} (DeLauder et al., 1992), whereas the decrease for binding of NTC-antithrombin to high-affinity heparin is 4–10%, given an overall value of -42 kJ mol^{-1}.

Rapid kinetic analysis of heparin binding to NTC-antithrombin

Stopped-flow experiments were used to determine the rapid kinetics of pentasaccharide binding to NTC-antithrombin. Previous studies have shown that pentasaccharide and high-affinity heparin bind to antithrombin in at least two steps (Olson et al., 1992), with the initial binding followed by a conformational change in antithrombin, converting it to a higher-affinity state for heparin.

$$\mathrm{AT} + \mathrm{H} \overset{K_1}{\rightleftharpoons} \mathrm{AT\text{-}H} \underset{k_{-2}}{\overset{k_2}{\rightleftharpoons}} \mathrm{AT\text{-}H^*}.$$

As shown, the initial binding equilibrium is defined by K_1, whereas the forward and reverse rate constants for the conformational change, which yields the fluorescence change, are defined by k_2 and k_{-2}, respectively. The curve at I0.15 for pentasaccharide binding (Fig. 2) yields a K_1 for the NTC-antithrombin–pentasaccharide interaction, which is 1.7-fold smaller than that for intact antithrombin, whereas the k_2 value for the NTC-antithrombin–pentasaccharide interaction is only slightly higher than that for intact antithrombin (Table 1).

The estimate of k_{-2} provided by nonlinear regression analysis has been found to be quite inaccurate (Olson et al., 1992) and is better estimated by the initial linear curve. This provides the association rate constant for the entire reaction, $k_{on} = k_2/K_1$, from the slope and the dissociation rate constant, $k_{off} = k_{-2}$, from the y-intercept. The latter is also difficult to estimate at I0.15 (Olson et al., 1992), thus the initial linear curve was repeated at I0.3. Due to limitations in the amount of high-affinity heparin, it was not possible to investigate the effects of higher concentrations, consequently only the initial linear curves are presented for this heparin species. The k_{on} for pentasaccharide binding to NTC-antithrombin at I0.15 was only slightly increased compared to the value for intact antithrombin, whereas the k_{off} was increased 12-fold (from inset of Fig. 2). However, with high-affinity heparin, both the k_{on} and k_{off} were increased for the interaction with NTC-antithrombin, with the former being 6.7-fold greater and the latter 8-fold greater than that for intact antithrombin at I0.15. At I0.3, the k_{on} for the NTC-antithrombin–pentasaccharide interaction was also similar to that for intact antithrombin, whereas the k_{off} was increased 4-fold. The k_{on} for high-affinity heparin binding to NTC-antithrombin at I0.3 was 2-fold greater and the k_{off} 10-fold higher than the values for intact antithrombin. Therefore, at both ionic strengths, similar patterns are seen, with the k_{on} for NTC-antithrombin–pentasaccharide interaction similar to that for intact antithrombin, whereas the k_{off} is greater, with both values increased for high-affinity heparin (Table 1).

Discussion

Selective cleavage of antithrombin by thermolysin at the Lys 29–Ala 30 bond has generated a form in which inhibitory activity was retained, whereas heparin affinity was lowered such that it eluted from heparin-Sepharose at an intermediate position between reactive site loop-cleaved (low affinity) antithrombin and intact (normal affinity) antithrombin. When antithrombin is cleaved at residue 29, the change in structure would be predicted to affect the segment from residues 22 to 46 (segment 22–46). This is due to stabilization of the segment from residues 1 to 21 by two disulfide bonds

Table 1. *Equilibrium dissociation constants, free energy changes and kinetic constants for heparin binding to NTC-antithrombin compared to those for intact antithrombin*

		$K_{d\,obs}$ (nM)	$\Delta\Delta G_b$ (kJ·mol^{-1})[a]	K_1 (μM)	k_2 (s^{-1})	k_{on} (μM^{-1} s^{-1})	k_{off} (s^{-1})
Heparin pentasaccharide							
0.15I	NTC-ATIII	199 ± 8	3.2	12.1 ± 1.1	632 ± 27	44.3 ± 2.4	7.0 ± 1.7
	α-ATIII	55.8 ± 4.8		20.4 ± 3.0	554 ± 53	38.7 ± 1.6	0.6 ± 0.7
0.3I	NTC-ATIII	1,481 ± 69	2.4			14.4 ± 1.0	26.2 ± 4.5
	α-ATIII	554 ± 41				11.6 ± 0.4	6.6 ± 0.5
High-affinity heparin							
0.15I	NTC-ATIII	20.8 ± 2.5	1.8			62.2 ± 3.2	6.1 ± 1.7
	α-ATIII	10.1 ± 1.4				9.3 ± 0.7	0.8 ± 0.2
0.3I	NTC-ATIII	145.3 ± 11.0	4			7.5 ± 0.4	5.0 ± 0.4
	α-ATIII	28.9 ± 1.6				3.6 ± 0.1	0.8 ± 0.07

[a]Calculated using the equation $\Delta\Delta G_b = RT \cdot \ln[K_{d\,obs}\text{NTC-ATIII}/K_{d\,obs}\alpha\text{-ATIII}]$. Values are given ± standard errors.

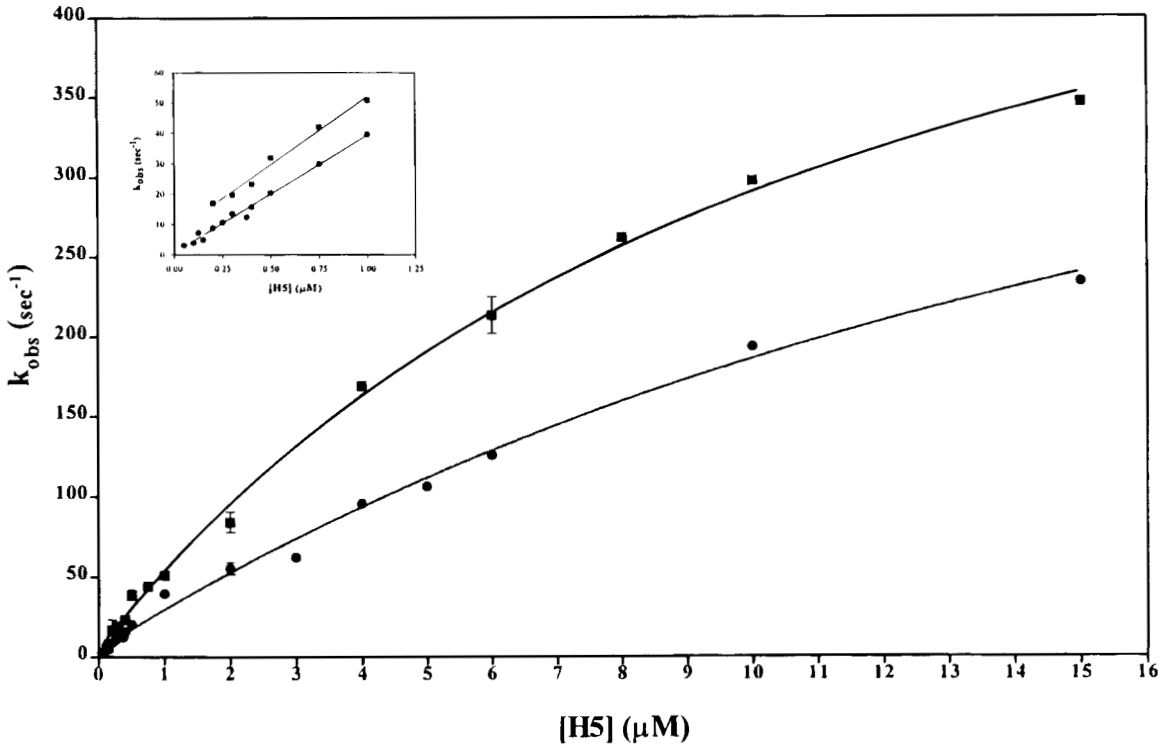

Fig. 2. Observed pseudo-first-order rate constants from pentasaccharide binding to NTC-antithrombin compared to intact antithrombin. Average k_{obs} values were measured by mixing pentasaccharide with NTC-antithrombin in the stopped-flow fluorimeter, where the heparin concentrations were at least fivefold greater than the antithrombin concentration, in I0.15 sodium phosphate buffer, pH 7.4, at 25 °C. The increase in intrinsic protein fluorescence accompanying binding was monitored and fit by nonlinear regression to a single exponential function to yield k_{obs} values for NTC-antithrombin (■) and intact antithrombin (●). Inset: Average k_{obs} values obtained at low heparin pentasaccharide concentrations, as above, for NTC-antithrombin (■) and intact antithrombin (●) fitted by linear regression.

(Fig. 3), between residues Cys 8–Cys 128 and Cys 21–Cys 95 (Carrell et al., 1994; Schreuder et al., 1994; Skinner et al., 1997). Because disruption in the segment constituting residues 22–46, by cleavage, yields a form with lowered affinity on heparin-Sepharose, it indicates that these residues are involved in the binding of heparin. This disruption to a defined area presented an opportunity to characterize the contribution of this region to the heparin binding interaction.

It was, however, important to assess whether cleavage at the N terminus caused any changes to the principal functions of the antithrombin molecule. An estimation based on the fluorescence change induced by heparin binding to intact and N-terminally modified antithrombin showed that there was a 9% decrease in the fluorescence emission relating to an alteration in the overall conformational change in NTC-antithrombin. This decrease in the overall conformational change appears to leave the inhibitory activity of the molecule unaffected, however, as judged from the fact that NTC-antithrombin inhibits factor Xa with a similar second-order rate constant to that of native antithrombin. Transmission of the conformational change to the reactive site similarly seems to be normal because rate constants for factor Xa inhibition in the presence of heparin pentasaccharide were also unaffected. Because factor Xa is sensitive to the loop conformation of antithrombin, the results showing normal functioning in the presence and absence of the pentasaccharide strongly indicate that NTC-antithrombin functions normally in all areas except for heparin binding. Logically, therefore, the decrease in overall conformational change on binding heparin found for NTC-antithrombin must stem from disruption localized to the cleaved region. Additional to this, cleavage is prevented by the minimal pentasaccharide unit, suggesting that the segment is in some way interacting or very close to the pentasaccharide in the bound form.

The decrease in heparin affinity for NTC-antithrombin found on heparin-Sepharose chromatography was confirmed by determination of the K_d for its interaction with both heparin pentasaccharide and high-affinity heparin. The overall loss of binding energy for this form of antithrombin was calculated to be about 5–10% of the overall binding energy of the interaction. This shows the relative contribution that segment 22–46 makes to the heparin binding mechanism.

Analysis of the rapid kinetics of the interaction between heparin and NTC-antithrombin fits with the proposal that segment 22–46 slightly obscures the heparin binding site and thus, upon cleavage, the initial interaction of heparin is eased somewhat, giving rise to the observed decrease in the initial equilibrium binding constant (K_1) and the consequent increased association constant (k_{on}). This increase in initial coupling appears to be even greater for high-affinity heparin, but, because K_1 and k_2, which constitute the k_{on}, could not be determined for this species, it cannot be discounted that there is also some alteration in the conformational change. Throughout these studies, however, the increase in dissociation constant for NTC-antithrombin and heparin is the dominant effect, giving rise to the overall lowered heparin affinity.

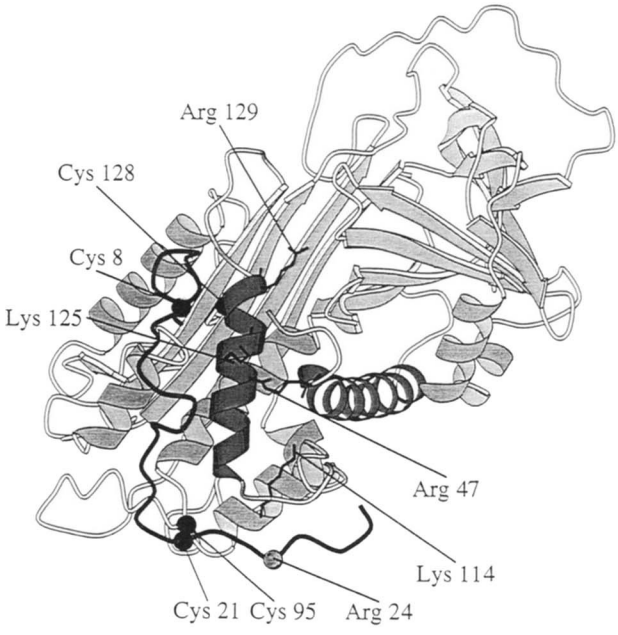

Fig. 3. Crystallographic structure of intact antithrombin. Intact antithrombin from the recently published 2.6-Å refinement of the crystallographic structure of active antithrombin, prepared using MOLSCRIPT (Kraulis, 1991), showing the D-helix and N-terminal segment of antithrombin from residue 1 to 29 highlighted in dark grey. Residues 29–42 are not present in the refinement of the structure because they are too disordered. The two disulfide bridges, Cys 8–Cys 128 and Cys 21–Cys 95, are shown as dark spheres, and the position of the residue mutated in antithrombin Rouen IV, Arg 24, is shown as a lighter sphere. The side chains of residues involved in pentasaccharide binding, Arg 47, Lys 114, Lys 125, and Arg 129, are shown in black.

In the crystallographic structure of the antithrombin, the segment from positions 29 to 42 is disordered (Carrell et al., 1994; Schreuder et al., 1994; Skinner et al., 1997), making a detailed structural interpretation of the biochemical data obtained somewhat difficult. The recently determined structure of antithrombin bound to the pentasaccharide (Jin et al., 1997) is also disordered from residues 26 to 38. Despite this lack of structural data, a comparison between the bound structure and that of unbound antithrombin (Fig. 4) is important in an explanation of why disruption to this area of the N terminus, by cleavage, affects pentasaccharide binding. Analysis of the two structures has shown that three areas of the pentasaccharide binding site, visible in the crystal structures, are subject to conformational change on binding; the D helix, which is elongated by one turn, the A helix, which is elongated by a half a turn, and the N-terminal residues 2–25 (Fig. 4). The end of the A helix is linked to the segment 22–46, and its elongation infers that the structurally unresolved residues must also move to accommodate this change (Fig. 4). An adjustment in this region in the N terminus of antithrombin, such as release of the segment by cleavage at residues 29–30, would predictably alter the character of the end of the A helix and lead to destabilization of the bound form, as shown by the dominant dissociation constant. This structural analysis supports the hypothesis that segment 22–46 participates in the conformational change and may even be a part of the driving force behind it, moving to allow the binding of heparin.

The N-terminal segment of antithrombin has been implicated previously in heparin binding due to its extended length compared to other serpins (Carrell et al., 1987) and the occurrence of low-affinity variants of antithrombin with mutations in this region, such as antithrombin Rouen IV (Arg 24 to Cys) (Borg et al., 1990) and antithrombin Basel (Pro 41 to Leu) (Chang & Tran, 1986). A

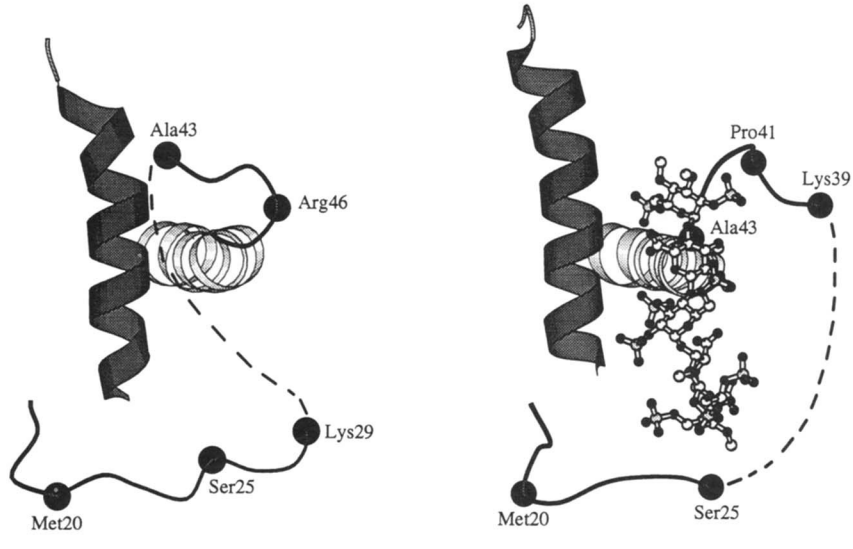

Fig. 4. Schematic drawings of the crystallographic structure of the pentasaccharide binding site in the bound and unbound forms of antithrombin. This figure shows the steric gate-like rearrangement of residues 22–46 that occurs when the pentasaccharide binds, moving aside to allow binding and stabilizing the bound form, prepared using MOLSCRIPT (Kraulis, 1991). Left: The 2.6-Å refinement of the crystallographic structure of active antithrombin (Skinner et al., 1997), showing the D helix in dark grey and the A helix in light grey. The N-terminal segment is shown in black with the area visible in the structure shown as a solid line and the area undefined, due to high mobility, shown as a broken line. Residues 43–46 adopt a coiled conformation to hinder access to the binding site. Right: The 2.9-Å refinement of the crystallographic structure of pentasaccharide-bound antithrombin (Jin et al., 1997) showing the elongated D helix in dark grey and the elongated A helix in light grey. The N-terminal segment is shown in black with the residues visible in the structure as a solid line and those not visible shown as a broken line. The pentasaccharide structure is shown in the ball and stick motif. Residues 39–44 can be seen to move to accommodate the pentasaccharide.

synthesis of the biochemical and crystallographic data available indicates that segment 22–46 initially impedes binding of heparin (an impediment which is removed upon cleavage with thermolysin, giving rise to the tighter initial binding seen here) and moves aside to allow binding of the heparin. Following this, the biochemical evidence suggests that the new position of segment 22–46 then participates in stabilizing the complex between heparin and antithrombin. Cleavage of the N-terminal segment would therefore prevent it from acting in concert with the rest of the molecule during the conformational change and not allow it to move to a position that stabilizes the interaction with the polysaccharide. Segment 22–46 may therefore be viewed as a steric gate that must be opened to allow heparin binding, following which, it moves to enclose the heparin into the binding pocket.

Materials and methods

Materials

Thermolysin was purchased from Sigma (UK). Heparin pentasaccharide was a gift from Maurice Petitou, Sanofi Research (France). High-affinity heparin was prepared after initial size fractionation of a porcine mucosal heparin preparation (Grampian Enzymes) using Sephadex G-100 (Laurent et al., 1978), to yield an approximately 7.8-kDa molecular weight fraction, which was then used to prepare the high-affinity fraction by adsorption to antithrombin-Sepharose, exactly as described (Olson et al., 1993). Factor Xa was purchased from Boehringer-Mannheim (UK). Thrombin was a gift from Professor Stuart Stone, Department of Biochemistry, Monash University, Melbourne. α-Antithrombin was prepared from time-expired human plasma as described (McKay, 1981). The chromogenic substrates S2222 and S2238 were purchased from Quadratech (UK).

Preparation of NTC antithrombin

NTC-antithrombin was prepared by incubating antithrombin (5 mg/mL) with thermolysin at a molar ratio of 400:1, in 20 mM Tris-HCl, 2 mM $CaCl_2$, pH 7.2, at 37 °C for 30 min, following which the thermolysin was inactivated by the addition of 10 mM EDTA. Cleavage was also performed as above in the presence of a 5-fold molar excess of pentasaccharide. The antithrombin (from cleavage in the absence of pentasaccharide) was equilibrated into 50 mM Tris-HCl, 10 mM trisodium citrate, 5 mM EDTA, 0.02% (w/v) NaN_3, pH 7.4 (buffer A), using centrifugal ultrafiltration and was bound to a heparin-Sepharose column (1.6 cm × 30 cm = 60 mL) equilibrated in buffer A and eluted using a linear salt gradient to 2 M NaCl in buffer A. The three forms so obtained were separately concentrated, buffer exchanged into 20 mM Tris-HCl, pH 7.4 (buffer B), and loaded onto a 5-mL HiTrap Q® column (Pharmacia), equilibrated in buffer B. These were eluted with a 30-mL gradient in buffer B to 0.5 M NaCl and separately concentrated and buffer exchanged into buffer A. For N-terminal sequence analysis, samples of antithrombin cleaved in the presence and absence of pentasaccharide were separated by non-reducing SDS-PAGE using the Tris/Tricine buffer system (Shagger & von Jagow, 1987) and blotted onto PVDF membrane (Matsudaira, 1987). The N-terminal sequence of each sample was determined by the Department of Biochemistry, University of Cambridge, on an Applied Biosystems 477A protein sequencing system. For mass spectrometry, purified samples were analyzed by the Department of Biochemistry, University of Cambridge, on a Kratos Kompact MALDI 4 V5.2.2 mass spectrometer.

Experimental conditions

All kinetic experiments were performed in a 20 mM NaH_2PO_4, 0.1% (w/v) PEG 8000, 0.1 mM EDTA, pH 7.4 buffer with the addition of 0.1 M NaCl or 0.25 M NaCl to give ionic strengths of 0.15 (I0.15) or 0.3 (I0.3), respectively.

Kinetic assays

The activity of antithrombin from chromatography eluates was tested by measuring the residual activity of 2 nM thrombin against 40 μM S2238, after incubation with 5 μL of each fraction for 2 h. Antithrombin concentrations were estimated by titration against thrombin of known concentration as described (Olson et al., 1993). Second-order rate constants of association for antithrombin inhibition of factor Xa were measured under pseudo-first-order conditions in a discontinuous assay (Olson et al., 1993), in the presence and absence of a 100-fold molar excess of pentasaccharide over antithrombin, with all incubations being performed at 37 °C.

Binding studies

Fluorescence emission spectra were determined exactly as described previously (Olson et al., 1992). Equilibrium dissociation constants for pentasaccharide and high-affinity heparin were determined by following the enhancement of intrinsic fluorescence during polysaccharide titrations as described previously (Olson et al., 1993). The concentration of NTC-antithrombin in titrations with pentasaccharide was 100 nM, whereas that used for high-affinity heparin was 50 nM. At least 40 titrations were performed and each experiment was repeated twice to obtain error values. Stopped-flow measurements of the kinetics of binding of high-affinity heparin and pentasaccharide to antithrombin were made on an Applied Photosystems stopped-flow apparatus, as described previously (Olson et al., 1981). Measurements were made under pseudo-first-order conditions, with heparin concentrations at least 5-fold greater than antithrombin. The increase in intrinsic protein fluorescence was monitored at emission wavelengths above 300 nm after excitation at 280 nm, at 25 °C, to give results that were fitted by a single exponential function, yielding k_{obs} values for the interaction at each heparin concentration. At least 16 sets of data were summed and each experiment was repeated to obtain k_{obs} and error values, which were then analyzed by nonlinear regression to obtain the individual constants.

Acknowledgments

We acknowledge the contributions of our late colleague, Professor Stuart Stone, to our understanding of the kinetics and techniques involved in this study and Professor Robin Carrell for continuing support and advice. We thank Dr. Len Packman of the Department of Biochemistry, University of Cambridge, for the protein sequencing and mass spectrometry performed. The work was supported by a Wellcome Trust, the British Heart Foundation, and the Medical Research Council.

References

Borg JY, Brennan SO, Carrell RW, George P, Perry DJ, Shaw J. 1990. Antithrombin Rouen-IV (24 Arg→Cys). The amino-terminal contribution to heparin binding. *FEBS Lett 266*:163–166.

Carrell RW, Christey PB, Boswell DR. 1987. Serpins: Antithrombin and other inhibitors of coagulation and fibrinolysis: Evidence from amino acid sequences. In: Verstraete M, Vermylen J, Lijnen HR, Arnout J, eds. *Thrombosis and haemostasis*. Leuven: Leuven University Press. pp 1–15.

Carrell RW, Stein PE, Fermi G, Wardell MR. 1994. Biological implications of a 3 Å structure of dimeric antithrombin. *Structure 2*:257–270.

Chang JY, Tran TH. 1986. Antithrombin III Basel. Identification of a Pro-Leu substitution in a hereditary abnormal antithrombin with impaired heparin cofactor activity. *J Biol Chem 261*:1174–1176.

Chang WS, Wardell MR, Lomas DA, Carrell RW. 1996. Probing serpin reactive-loop conformations by proteolytic cleavage. *Biochem J 314*:647–653.

Choay J, Petitou M, Lormeau JC, Sinay P, Casu B, Gatti G. 1983. Structure–activity relationship in heparin: A synthetic pentasaccharide with high affinity for antithrombin III and eliciting high anti-factor Xa activity. *Biochem Biophys Res Commun 116*:492–499.

DeLauder S, Schwarz FP, Williams JS, Atha DH. 1992. Thermodynamic analysis of heparin binding to human antithrombin. *Biochem Biophys Acta 1159*:141–149.

Hunt LT, Dayhoff MO. 1980. A surprising new protein superfamily containing ovalbumin, antithrombin III and α_1-proteinase inhibitor. *Biochem Biophys Res Commun 95*:864–871.

Jin L, Abrahams JP, Skinner R, Petitou M, Pike RN, Carrell RW. 1997. The anticoagulant activation of antithrombin by heparin. *Proc Natl Acad Sci USA 94*:14683–14688.

Kraulis P. 1991. MOLSCRIPT: A program to produce both detailed and schematic plots of proteins. *J Appl Crystallogr 24*:946–950.

Laurent TC, Tengblad A, Thunberg L, Höök M, Lindahl U. 1978. The molecular-weight-dependence of the anti-coagulant activity of heparin. *Biochem J 175*:691–701.

Matsudaira P. 1987. Sequence from picomole quantities of proteins electroblotted onto polyvinylidene difluoride membranes. *J Biol Chem 262*:10035–10038.

McKay EJ. 1981. A simple two-step procedure for the isolation of antithrombin III from biological fluids. *Thromb Res 21*:375–382.

Olson ST, Björk I. 1992. Regulation of thrombin by antithrombin and heparin cofactor II. In: Berliner LJ, ed. *Thrombin: Structure and function*. New York: Plenum Press. pp 159–217.

Olson ST, Björk I, Sheffer R, Craig PA, Shore JD, Choay J. 1992. Role of the antithrombin-binding pentasaccharide in heparin acceleration of antithrombin–proteinase reactions. Resolution of the antithrombin conformational change contribution to heparin rate enhancement. *J Biol Chem 267*:12528–12538.

Olson ST, Björk I, Shore JD. 1993. Kinetic characterization of heparin-catalyzed and uncatalyzed inhibition of blood coagulation proteinases by antithrombin. *Methods Enzymol 222*:525–559.

Olson ST, Srinivasan KR, Björk I, Shore JD. 1981. Binding of high affinity heparin to antithrombin III. Stopped flow kinetic studies of the binding interaction. *J Biol Chem 256*:11073–11079.

Schreuder HA, de Boer B, Dijkema R, Mulders J, Theunissen HJM, Grootenhuis PDJ, Hol WGJ. 1994. The intact and cleaved human antithrombin III complex as a model for serpin–proteinase interactions. *Nature Struct Biol 1*:48–55.

Shagger H, von Jagow G. 1987. Tricine-sodium dodecyl sulphate-polyacrylamide gel electrophoresis for the separation of proteins in the range from 1 to 100 kDa. *Anal Biochem 166*:368–379.

Skinner R, Abrahams JP, Whisstock JC, Lesk AM, Carrell RW, Wardell MR. 1997. The 2.6 Å structure of antithrombin indicates a conformational change at the heparin binding site. *J Mol Biol 266*:601–609.